

Rheology of concentrated biomass

J. R. Samaniuk¹, J. Wang¹, T. W. Root¹, C. T. Scott² and D. J. Klingenberg¹

¹Department of Chemical and Biological Engineering, and Rheology Research Center,
University of Wisconsin, Madison, WI 53706

²U.S. Forest Service Forest Products Laboratory, Madison, WI 53706

(Received October 14, 2011)

Abstract

Economic processing of lignocellulosic biomass requires handling the biomass at high solids concentration. This creates challenges because concentrated biomass behaves as a Bingham-like material with large yield stresses. Here we employ torque rheometry to measure the rheological properties of concentrated lignocellulosic biomass (corn stover). Yield stresses obtained using torque rheometry agree with those obtained using other rheometric methods, but torque rheometry can be used at much larger solids concentration (weight fractions of insoluble solids greater than 0.2). Yield stresses decrease with severity of hydrolysis, decrease when water-soluble polymers are added (for nonhydrolyzed biomass), and increase with particle length. Experimental results are qualitatively consistent with those obtained from particle-level simulations.

Keywords : biomass, corn stover, rheology, yield stress, viscosity

1. Introduction

Lignocellulosic biomass refining typically involves numerous steps. In a process developed by the National Renewable Energy Laboratory (NREL) for the conversion of corn stover to ethanol (Aden *et al.*, 2002; Schell *et al.*, 2003), the biomass is first “pretreated” using dilute acid hydrolysis at elevated temperature in order to make the cellulose more accessible. The cellulose is then enzymatically hydrolyzed to produce glucose. The glucose is subsequently fermented to produce an ethanol solution; the ethanol is then purified in several separation steps. Commercialization of such processes requires reducing the processing costs (Wooley *et al.*, 1999; Sheehan *et al.*, 2004; Wyman, 2007). In the Biofine process (Bozell *et al.*, 2000), biomass is hydrolyzed to hydroxymethylfurfural in a first reactor operated at 210–230°C. This material is then converted to levulinic acid in a second reactor operated at 195–215°C. Levulinic acid can be converted to a variety of chemicals and fuels (Bozell and Petersen, 2010; Serrano-Ruiz *et al.*, 2010a, 2010b).

The cost of processing biomass can be reduced by increasing the concentration of insoluble solids in the various operations (Lynd, 1996; Wingren *et al.*, 2003; Jorgensen *et al.*, 2007). Reduced water content decreases heating costs and can decrease equipment costs through reduced material volume. However, increasing the solid concentration increases the apparent viscosity of the bio-

mass, which makes mixing and transporting the biomass more challenging (Rosgaard *et al.*, 2007; Um and Hanley, 2008; Lu *et al.*, 2010). It is thus apparent that optimization of biomass processes will benefit from understanding the factors that affect the rheology of the biomass.

Lignocellulosic biomass is essentially a concentrated suspension of natural fibers. Considerable research has been reported on the rheological properties of wood fiber suspensions because of their importance in the pulp and paper industry. Although pulp and paper processing typically involves fiber concentrations much smaller than those anticipated for biorefining, research in pulp suspensions has provided considerable information about the factors that influence the rheology of natural fiber systems. The rheological properties of wood fiber suspensions depend on a variety of variables, including fiber concentration, fiber length, flexibility and fiber interactions.

The concentration of fiber suspensions can be characterized by the crowding number $N_c = 2r_p^2\phi/3$ (Kerekes and Schell, 1992; Dodson, 1996), which is the average number of fibers in a spherical volume of diameter equal to the fiber length L , where $r_p = L/d$ is the fiber aspect ratio, d is the fiber width, and ϕ is the fiber volume fraction. The concentrated regime is dened as $N_c > r_p$. This regime is the most challenging to study and model, and the most relevant to high-solids biomass processing. For fibers to form flocs or coherent networks, every fiber must be in contact with at least three other fibers (Dodson, 1996; Meyer and Wahren, 1964; Soszynski and Kerekes, 1988a). The number of contacts per fiber, n_{contacts} , has been

*Corresponding author: klingen@engr.wisc.edu
© 2011 The Korean Society of Rheology and Springer

related to the fiber concentration by (Dodson, 1996) $n_{\text{contact}} = 3N_c/r_p = 2r_p\phi$. Thus, to form a coherent network ($n_{\text{contact}} \geq 3$), one must have $N_c > r_p$, which provides a basis for dening the concentrated regime.

The strength of flocculated networks can be characterized by the elastic storage modulus G' obtained from small amplitude oscillatory shear measurements (Kurath, 1959). The storage modulus G' can be related to the solids concentration C by the empirical expression $G' = k(C - C_s)^z$ (Thalen and Wahren, 1964a, 1964b, 1964c), where C_s is the sedimentation concentration. Experiments reveal that z is typically in the range 1.5–3 for $C < 8$ wt% (Thalen and Wahren, 1964b; Swerin *et al.*, 1992). Meyer and Wahren (1964) extended a model for the elastic properties of paper sheet to fiber networks. Analytical expressions obtained for the fiber network shear modulus and sedimentation concentration qualitatively captured the dependence of the shear modulus on concentration and aspect ratio, and sedimentation concentration on aspect ratio.

Bergman and Takamura (1965) and Almin *et al.* (1967) found that the network shear strength increased with fiber stiffness. The sedimentation concentration also depended on fiber stiffness. These results are inconsistent with the model of Meyer and Wahren (1964), illustrating that the model does not correctly account for the influence of fiber flexibility. The importance of fiber flexibility was also illustrated by Soszynski and Kerekes (1988a, 1988b), who found that networks of nylon fibers could be dispersed more easily when the fiber stiffness was reduced by heating suspensions above the glass transition temperature of the nylon model fibers.

The strength of fiber suspensions can also be characterized by a yield stress—the stress required to cause the network to fail and generate flow. Bennington *et al.* (1990) measured the yield stress of wood pulp and synthetic fiber suspensions in a rotary viscometer. They found that the yield stress τ_0 scaled as a power-law in solids concentration,

$$\tau_0 = aC^b \quad (1)$$

as predicted by Meyer and Wahren (1964). The value of the exponent b ranged from 2.3 to 3.6 for different types of fibers. Similar concentration dependences have been reported by others (Swerin *et al.*, 1992; Dalpke and Kerekes, 2005; Kerekes, 2006). However, Bennington *et al.* (1990) observed a dependence of the yield stress on fiber aspect ratio and modulus of elasticity that did not agree with that predicted. They suggested that fiber bending alone did not account for the network strength as predicted by the network model.

Numerous studies have illustrated that certain water-soluble polymers (WSPs) can reduce the apparent viscosity of wood pulp suspensions (Singh, 1985; Lindstrom, 1989; Lin and Lindstrom, 1989; Zauscher, 1999; Zauscher *et al.*, 2000). We have found that by adding various WSPs, slur-

ries at high solids concentrations (up to 50% fibers by volume) can be made to flow homogeneously with only a few wt% polymer (Scott, 2002). Using this approach, high concentration fiber slurries can be extruded using equipment commonly employed in the food and plastics processing industries (Zauscher, 1999; Zauscher *et al.*, 2000). Using colloidal probe microscopy (CPM) to investigate the effects of WSPs in model fiber contacts, we have found that the WSPs act primarily by significantly reducing the coefficient of sliding friction between the cellulose surfaces (Zauscher, 1999; Zauscher and Klingenberg, 2000, 2001a, 2001b).

As might be expected, rheological properties of biomass targeted for fuels and chemicals are similar to those of paper pulp slurries. Pimenova and Hanley (2003, 2004) measured the apparent rheological properties of pretreated corn stover suspensions (average fiber length 120 μm) using a Brookeld viscometer with a helical impeller. The shear stress-shear rate data exhibited plastic-type rheological behavior with an apparent yield stress. The yield stress increased with solids concentration, but no information about the dependence of rheological properties on pretreatment conditions was reported. The authors also noted that the helical impeller technique is not appropriate for concentrated slurries (solids mass fraction > 32%).

Rosgaard *et al.* (2007) investigated the effect of solid content and enzymatic hydrolysis on the apparent viscosity of barley straw biomass slurries, with solid mass fractions varying from 5 to 15 wt%. The apparent viscosity increased with solid mass fraction, and decreased with time during enzymatic hydrolysis.

More recently, Viamajala *et al.* (2009) examined the rheology of acid hydrolyzed corn stover at high solids concentrations (10–40 wt%) using a Brookeld viscometer with parallel disks. The corn stover was finely milled using a Wiley mill. The authors also found that the corn stover slurries behaved like yield stress fluids, with yield stresses that decrease with increasing hydrolysis temperature and decreasing particle size. The authors also found that the yield stress increased with solids concentration up to a point, and then became independent of concentration at high concentrations. The reason for the plateau at high concentrations is not clear.

Knutsen and Liberatore (2009) also examined the rheology of dilute acid hydrolyzed corn stover using a variety of techniques. Measurements with parallel disks were fraught with a variety of problems, including wall slip (for smooth disks), results sensitive to the normal load, and fracture and ejection. These phenomena may explain in part the unexpected yield stress plateau at high solids concentrations reported by Viamajala *et al.* (2009). Knutsen and Liberatore were able to make more reproducible measurements using a vane geometry. Yield stresses were extracted for insoluble solids concentrations up to about

17 wt%. The concentration dependence of the yield stress was fit with Eq. 1, resulting in an exponent of $b = 6.0 \pm 0.4$. Stickel *et al.* (2009) also measured yield stresses on similar hydrolyzed materials using a variety of techniques. Again, the yield stress data were well described by Eq. 1 with an exponent of $b = 5.7 \pm 0.5$.

The rheometric techniques and geometries described above are limited to biomass with low to moderate concentrations. The main limitations to the parallel disk geometry include slip, fracture, ejection and sensitivity to the normal load applied to the plates. For the vane geometry, the main limitation is the inability to insert the vane without compressing the biomass when the yield stress is large. Torque rheometry is another technique which can be employed when the materials have such large yield stresses. This method has been used to determine the processability of rheologically challenging materials ranging from foods to polymers (Goodrich and Porter, 1967; Blyler and Daane, 1967; Steffe, 1996; Connelly and Kokini, 2004). Torque rheometers measure the mechanical resistance of the sample being mixed. By calibrating the rheometer with known materials (Goodrich and Porter, 1967; Blyler and Daane, 1967), the measured quantities can be converted to conventional rheological quantities such as the shear stress and viscosity.

In this article, we describe how torque rheometry can be used to measure rheological properties of highly concentrated biomass. We compare values of the yield stress measured using this technique with values obtained using other methods. We then examine the concentration dependence of the yield stress of a variety of different systems. Finally, we show how the experimental results are consistent with recent simulation results.

2. Experimental

2.1. Materials

Baled corn stover was hammermilled, washed and dewatered. The hammermilled corn stover had a distribution in particle sizes ranging from centimeters to micrometers. Some experiments were performed with dilute-acid hydrolyzed corn stover. The hydrolysis methods are described elsewhere (Ehrhardt, 2008; Ehrhardt *et al.*, 2010). Carboxymethyl cellulose (Aqualon 7H4F) was employed in some experiments; the use of such water soluble polymers to improve rheological properties of biomass is described elsewhere (Samaniuk *et al.*, 2011).

2.2. Vane rheometry

A vane geometry was fabricated for use with a Bohlin VOR rheometer (Monz, 2009). The vane consists of four blades placed in an outer cylinder with six baffles. Yield stresses are determined using the maximum torque method (Dzuy and Boger, 1983, 1985). Here, the outer cylinder is

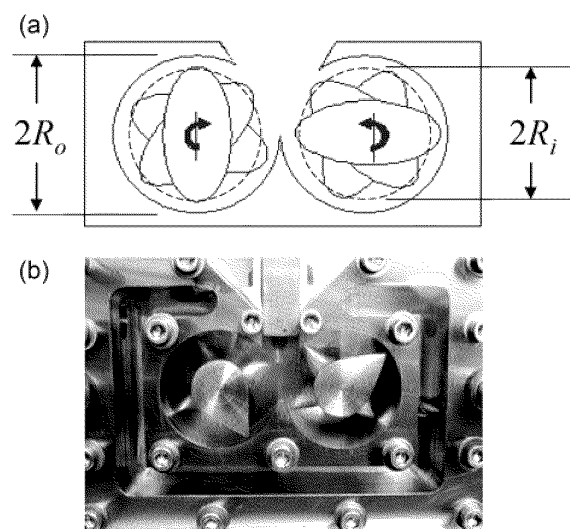


Fig. 1. (a) Schematic diagram of the torque rheometer. (b) Photograph of the torque rheometer chamber. The right impeller rotates at 2/3 the speed of the left impeller.

rotated slowly while the torque exerted on the vane is measured. The torque increases with time, passes through a maximum, and then decreases. The maximum torque, Γ_{\max} , is insensitive to the rotation rate for sufficiently low rates. The yield stress is equated with the shear stress at the outer edge of the vane. When the biomass fills the outer cylinder to the top of the vane (as opposed to immersing the vane completely), an analysis similar to those in Dzuy and Boger (1983, 1985) yields the formula for the yield stress

$$\tau_0 = \frac{2}{\pi D^3} \left(\frac{L}{D} + \frac{1}{6} \right)^{-1} \Gamma_{\max} \quad (2)$$

where D and L are the vane diameter and length, respectively.

2.3. Torque rheometry

Torque rheometry was performed using a modified Brabender Plasticorder, illustrated in Fig. 1. The rheometer consists of a metal mixing chamber with two equally sized cylindrical volumes where chrome-plated steel impellers counter-rotate to impose shear on the biomass. Between the cylindrical shear zones, there is a mixing zone where material can pass from one cylinder to the other. One impeller rotates at the input shaft speed (impeller 1) while the other turns at 2/3 of the input speed (impeller 2). The temperature of the mixing chamber is controlled by water flowing through a channel around the chamber. Total shaft torque is measured with a magnetoelastic sleeve torque transducer connected to the motor shaft and recorded at 5 Hz. Both water temperature and chamber internal temperature are measured using thermocouples, with the internal chamber thermocouple enclosed in a thermowell

inserted into the top of the chamber.

To perform rheological measurements, the mixing chamber is completely filled with the test material. During sample addition, the shaft is turned by hand to expose air bubbles, which are then removed by adding more material. Once the chamber is full, the water temperature is adjusted to attain the desired test temperature. Mixing and data acquisition for torque and temperature begin when the internal temperature is within 5°C of the target temperature, as mixing causes the internal temperature to equilibrate rapidly.

For the experiments reported here, the torque rheometer measurements were performed as follows. The input shaft speed was first maintained at 110 rpm for 600 s. This step is employed to help reach a steady measured torque. The input shaft speed was then cycled through a series of steps, with increasing and decreasing shaft speeds: the speed was held for 100 seconds at each of 55, 110, 220, 110, and 55 rpm to obtain torque data at each of these rotation rates. This sequence of steps was repeated two to four times (other input speeds, such as 28 and 165 rpm, were occasionally added to the sequence of steps). Unless specifically stated otherwise, measurements were performed at 55°C.

The effect of rheometer temperature on rheological properties was investigated in some runs. Immediately after the step sequence described above, the temperature was changed to different steady values and the torque was measured for a sequence of decreasing shaft speeds.

Torque-rotation rate data were converted to conventional rheological quantities using a calibration procedure developed by Goodrich and Porter (1967). The torque rheometer is represented by two sets of concentric cylinders. The outer cylinder radius, R_o , is equated with the actual cylindrical bowl radius. The effective inner radius, R_i , is determined by equating the measured torque for a Newtonian fluid with known viscosity with that calculated from the solution of the Navier-Stokes equation (Ehrhardt, 2008). Bousmina *et al.* (1999) showed that such a calibration with a Newtonian fluid gives equivalent results to that obtained using a more sophisticated analysis with power-law fluids.

Once the effective inner radius is obtained, the torque (Γ) and rotation rate (Ω) data can be transformed into apparent shear stress (τ) and apparent shear rate ($\dot{\gamma}$) data for the fast impeller (impeller 1) for a torque rheometer with a 3:2 drive-to-driven gear ratio via

$$\tau = \frac{9}{132\pi R_a^2 h} \Gamma \quad (3)$$

$$\dot{\gamma} = \frac{2R_i R_o \Omega}{\left(\frac{1}{\kappa} - \kappa\right) R_a^2} \quad (4)$$

where $R_a = (R_i + R_o)/2$ is the midpoint radius, h is the impeller depth, and $\kappa = R_i/R_o$. This approach is consistent with

that employed in commercial rheometers (Bohlin). To extract rheological parameters such as a yield stress, one can simply fit the torque-rotation rate data with that predicted for a particular constitutive model. We follow this approach, employing the Bingham model, where the local stress τ_{loc} is related to the local shear rate $\dot{\gamma}_{loc}$ by

$$\tau_{loc} = \tau_0 + \eta_{pl} \dot{\gamma}_{loc} \quad (5)$$

where τ_0 is the yield stress and η_{pl} is the plastic viscosity. The predicted torque is $\Gamma = \Gamma_1 + (2/3)\Gamma_2$, where the torque-rotation rate relationship for concentric cylinder geometry k is ($k = 1, 2$)

$$\Gamma_k = 4\pi R_i^2 h \left[\frac{\Omega_k + \frac{\tau_0}{\eta_{pl}} \ln\left(\frac{r_0}{R_i}\right)}{1 - \frac{R_i^2}{r_0^2}} \right], \quad (6)$$

and where r_0 is the location of the radius at which the velocity goes to zero, determined by solution of

$$\left(\frac{r_0}{R_i}\right)^2 - 1 = \frac{2\eta_{pl}\Omega_k}{\tau_0} + \ln\left[\left(\frac{r_0}{R_i}\right)^2\right] \quad (7)$$

For $r_0 > R_o$, the torque is given by Eq. 6 with r_0 replaced by R_o . Thus by fitting the above model for the predicted torque to experimental torque-rotation rate data, the yield stress and plastic viscosity can be extracted. For this fitting procedure, we employ a Gauss-Newton method to minimize the error between the measured and predicted torques (Ehrhardt, 2008). We note that Eqs. 6 and 7 reveal that for the torque rheometer geometry, the torque is not a linear function of the rotation rate for the Bingham model, and therefore the apparent shear stress (Eq. 3) is not a linear function of the apparent shear rate (Eq. 4).

2.3.1. Fiber-level simulations

Yield stresses obtained experimentally were compared with those obtained using fiber-level simulations. In these shear flow simulations, flexible fiber suspensions are modeled as neutrally-buoyant, linked, rigid bodies immersed in a Newtonian liquid. Here we briefly describe the model and simulation method; more details can be found elsewhere (Switzer, 2002; Switzer and Klingenberg, 2003). Each fiber is represented by N_{seg} rigid cylinders (length $2R$, radius b , overall fiber length $L = 2RN_{seg}$) with hemispherical end caps, connected end-to-end by ball and socket joints. The motion of each fiber segment is described by Newton's equations of translational and rotational motion, in which we neglect fluid and fiber inertia. The evolution of the fiber shapes, orientations and positions in flow are simulated by numerically integrating the equations of motion subject to the forces and torques acting on each segment. Forces and torques acting on the fibers include: constraint forces that maintain the con-

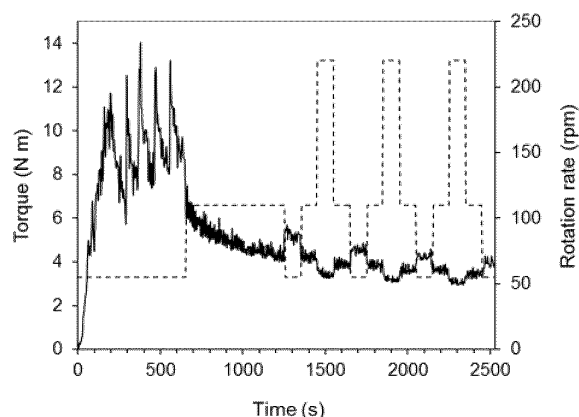


Fig. 2. Torque (solid curve) and rotation rate (dashed curve) as a function of time for 25 wt% hammermilled corn stover at 35°C.

nectivity of the segments within each fiber; hydrodynamic forces and torques; bending and twisting potentials within the hinges to resist fiber deformation; short-range repulsive forces to prevent fiber overlap; and friction between fibers in contact. Hydrodynamic forces and torques are treated in the free-draining, zero Reynolds number limit. Bending and twisting torques are assumed to be linear in the deviations of the bending and twisting angles (θ and ϕ) from their equilibrium values (θ^{eq} and ϕ^{eq}), with bending and twisting spring constants $k_b = E_Y I / 2R$ and $k_t = E_Y J / 2R$ (E_Y is the fiber Young's modulus, and I and J are the corresponding moments of inertia). For all results reported here, $k_t = 0.67k_b$, mimicking a linearly elastic circular cylinder with a Poisson's ratio of 0.5. The fiber stiffness is characterized by the dimensionless effective stiffness, $S^{eff} \equiv E_Y I / \eta_0 \dot{\gamma} L^4$, where η_0 is the suspending fluid viscosity, and $\dot{\gamma}$ is the shear rate. Friction forces are characterized by a static coefficient of friction μ^{stat} . Shear stresses are calculated in a conventional manner (Switzer and Klingenberg, 2003). Yield stresses are obtained by extrapolating shear stress-shear rate data to zero shear rate.

3. Results

3.1. Torque rheometry

Typical torque rheometry results are illustrated in Fig. 2, where torque and rotation rate are plotted as a function of time for 25 wt% hammermilled corn stover at 35°C. The torque fluctuates considerably during the loading phase ($t < 650$ s). After the loading phase, the input shaft is rotated at 110 rpm for 600 s ($650 < t < 1250$ s). The torque decreases with time during this phase as the average particle size is slowly reduced. The speed is then cycled up and down several times, eventually generating reproducible time-averaged torques at various rotation rates.

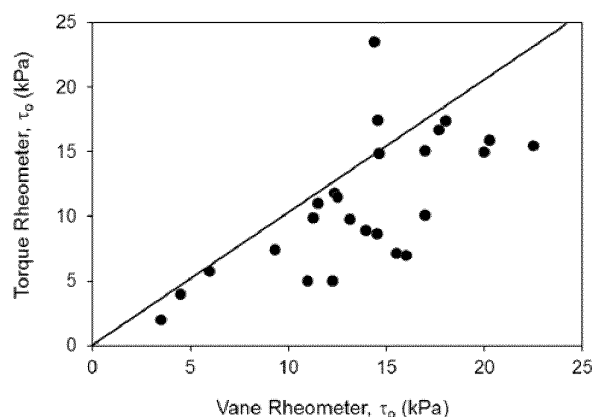


Fig. 3. Yield stress obtained using the torque rheometer vs the yield stress obtained using the vane geometry for various corn stover samples.

3.2. Comparison of yield stresses measured with different instruments

If the solids concentration is not too large, or if the biomass has been sufficiently hydrolyzed, or if rheological modifiers have been added, the yield stresses of biomass samples can be sufficiently small such that they can be measured using both the torque rheometer and the vane rheometer. Yield stresses obtained using both the torque rheometer and the vane rheometer are compared for various corn stover samples in Fig. 3. The data here represent a wide variety of corn stover materials—untreated hammermilled slurries at low solids concentrations, materials acid-hydrolyzed at various concentrations, and hammermilled corn stover at various concentrations whose yield stresses have been reduced by the addition of water-soluble polymers. For all of these materials, the different measurement techniques produce similar values for the yield stress, although vane rheometry with the maximum torque method tends to give slightly larger values for the yield stress.

Stickel *et al.* (2009) measured the yield stress of an acid hydrolyzed corn stover material using a variety of techniques, and compared the values obtained over a wide range of concentrations. The rheometric approaches included a maximum stress method using oscillatory flow with parallel disks, the maximum stress method using a vane geometry, and the torque rheometry method described above. The results of that study are summarized in Fig. 4 where the yield stress is plotted as a function of insoluble solids concentration. As in Fig. 3, there is considerable scatter among the data obtained using the various techniques. However, the trend that the yield stress is a strong, increasing function of solids concentration is observed with all methods. Fitting all of the data with Eq. 1 gives a value of the exponent $b = 5.8 \pm 0.6$. Fig. 4 also illustrates that torque rheometry is the only technique for measuring yield stresses at the largest concentrations.

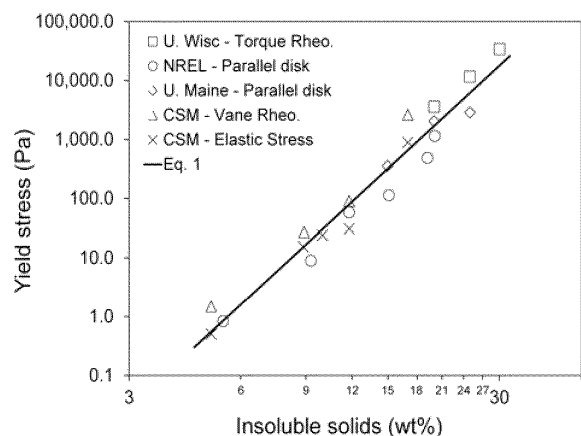


Fig. 4. Yield stress as a function of insoluble solids concentration for an acid hydrolyzed corn stover material, obtained using a variety of rheometric methods. Data obtained from Stickel *et al.* (2009).

3.3. Effects of acid hydrolysis conditions on yield stress

The yield stress of corn stover samples varies with the dilute acid hydrolysis reaction conditions. The yield stress of hammermilled corn stover samples is plotted as a function of solids concentration in Fig. 5(a), for different hydrolysis temperatures. In each case, the stover was heated in 1 wt% sulfuric acid for 30 min at the indicated effective reaction temperature (Ehrhardt *et al.*, 2010). As the effective reaction temperature is increased, the yield stress decreases. For each case, however, the yield stress still increases as a power-law function of solids concentration (the solid curves are fits of the data with Eq. 1). The exponent b is relatively insensitive to reaction temperature, with $3.7 < b < 4.3$ (Ehrhardt *et al.*, 2010).

Also shown in Fig. 5(a) are data for the yield stress of untreated, hammermilled corn stover. The yield stresses for these samples are significantly larger than those of the hydrolyzed samples. Although the yield stress increases with solids concentration, it is not described well by the power-law function. This is likely related to a smaller degree of size reduction with the lower concentration sample. In Fig. 5(b), the natural log of the yield stress is plotted as a function of the natural log of the solids concentration. Here the power-law fits appear as straight lines. When the lowest concentration data point for the untreated stover is omitted from the power-law fit, the power-law fit is more consistent with the power-law fits of the hydrolyzed materials.

3.4. Effects of rheological modifiers on yield stress

The yield stress of biomass can be controlled to some extent by the addition of rheological modifiers. Knutsen and Liberatore (2010) found that the yield stress of acid

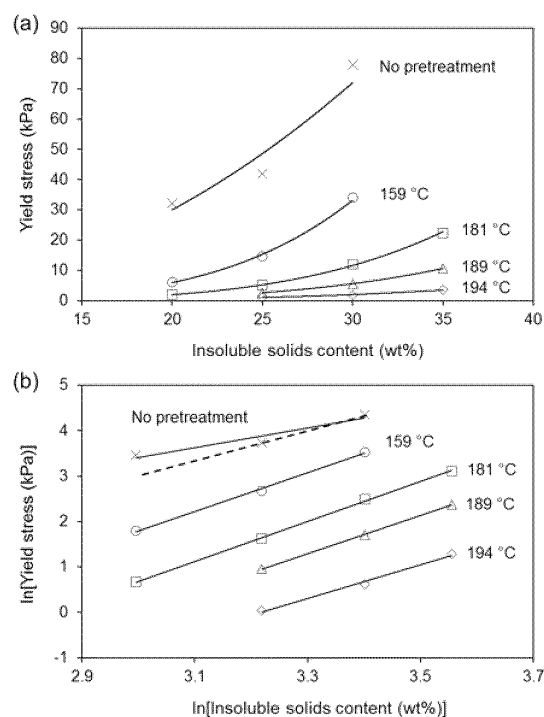


Fig. 5. (a) Yield stress as a function of insoluble solids concentration for hammermilled corn stover hydrolyzed in 1 wt% sulfuric acid for 30 min at different effective reaction temperatures. Data obtained from Ehrhardt *et al.* (2010) for the hydrolyzed materials, and from Samaniuk *et al.* (2011) for the untreated material. The solid curves represent fits with the power-law function (Eq. 1). (b) Same data replotted as the natural log of the yield stress vs the natural log of the concentration. The dashed curve is a power-law fit of the data for the untreated material with lowest concentration data point omitted.

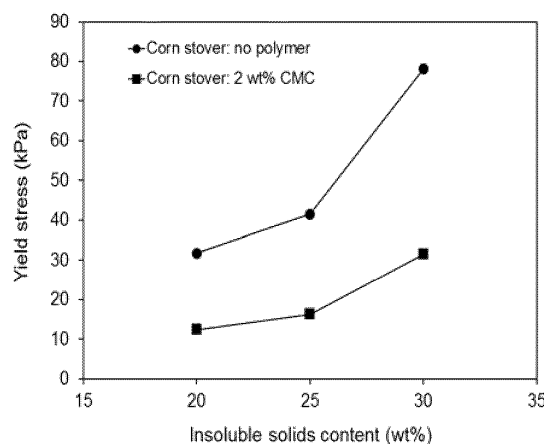


Fig. 6. Yield stress as a function of insoluble solids concentration for nonhydrolyzed, hammer-milled corn stover and switchgrass, with and without the addition of 2 wt% CMC (based on the dry weight of the biomass). Data obtained from Samaniuk *et al.* (2011).

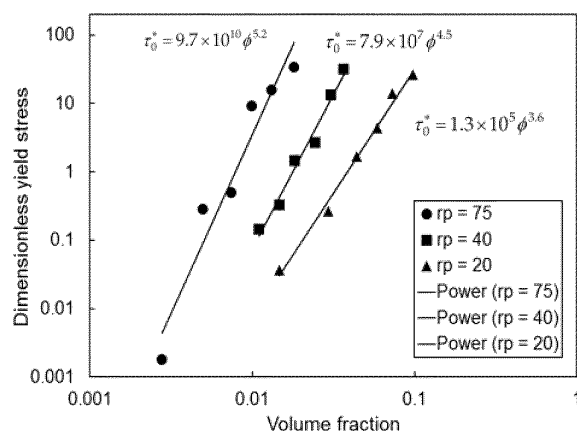


Fig. 7. Yield stress obtained from fiber-level simulations as a function of fiber volume fraction, for three fiber aspect ratios $r_p \equiv L/2b = L/d$.

hydrolyzed materials could be reduced by the addition of surfactants. We have found that the yield stress of non-hydrolyzed materials can be reduced by the addition of water-soluble polymers. This is illustrated in Fig. 6 where the yield stress is plotted as a function of solids concentration for corn stover with and without the addition of 2 wt% carboxymethyl cellulose (CMC; based on the dry weight of the biomass). The yield stress decreases significantly with the addition of the CMC, and the yield stress continues to increase with increasing solids content.

3.5. Yield stresses obtained via fiber-level simulations

The rheological properties of fiber suspensions such as biomass can also be investigated via fiber-level simulations. Simulations were performed for systems composed of U-shaped fibers ($\theta^q = 0.1, \phi^{eq} = 0$), of various aspect ratios and effective stiffnesses. For sufficiently large concentrations, these materials exhibited pseudoplastic behavior with an apparent yield stress. The yield stresses were extracted by fitting the dimensionless shear stress-shear rate data with the Bingham model (Wang, 2012). Yield stresses obtained in this manner are plotted as a function of fiber volume fraction in Fig. 7, for three different fiber aspect ratios. The yield stress increases with fiber aspect ratio, which is consistent with experimental results where the yield stress is an increasing function of fiber length (Bennington *et al.*, 1990; Samaniuk *et al.*, 2011). For each data set, the simulated yield stress follows the power-law dependence of Eq. 1. The values of the exponent b are similar in magnitude to the values obtained experimentally for the corn stover systems. The exponent increases weakly with aspect ratio, which is counter to that observed in two experimental studies with wood fiber suspensions. Dalpke and Kerekes (2005) and Derakshandeh *et al.* (2010) both

reported that yield stresses follow a power-law dependence on concentration, but that the exponent decreased slightly with increasing fiber length. In these cases, however, other fiber properties were not held constant, so it is unclear if the change in the exponent is caused by a change in fiber aspect ratio. It is likely that more experimental and simulation results will be required to understand the effects of fiber properties on yield stress.

4. Conclusions

Here we employ torque rheometry to measure the rheological properties of concentrated lignocellulosic biomass (corn stover). Yield stresses obtained using torque rheometry agree with those obtained using other rheometric methods, but torque rheometry can be used at much larger solids concentration (weight fractions of insoluble solids greater than 0.2). Yield stresses decrease with severity of hydrolysis, decrease when water-soluble polymers are added, and increase with particle length. Experimental results are qualitatively consistent with those obtained from particle-level simulations, where yield stresses increase as a power-law function of solids concentration.

Acknowledgments

This project was supported by the U.S. Department of Agriculture (NRI award number 2006-35504-17401 and AFRI award number 2010-65504-20406).

References

- Aden, A., M. Ruth, K. Ibsen, J. Jechura, K. Neeves, J. Sheehan, B. Wallace, L. Montague, A. Slayton, and J. Lukas, 2002, Lignocellulosic biomass to ethanol process design and economics utilizing co-current dilute acid prehydrolysis and enzymatic hydrolysis for corn stover, NREL Technical Report TR-510-32438.
- Almin, K. E., P. Biel, and D. Wahren, 1967, Relating the shear modulus of fibre networks to the bulk average fiber stiffness, *Svensk Papperstidn.* **70**, 772-774.
- Bennington, C., R. Kerekes, and J. Grace, 1990, The yield stress of fibre suspensions, *Can. J. Chem. Eng.* **68**, 748-757.
- Bergman, J. and N. Takamura, 1965, The correlation between the shear modulus of fibre networks and the individual fibre stiffness, *Svensk Papperstidn.* **68**, 703-710.
- Blyler, L. L. and J. H. Daane, 1967, An analysis of Brabender torque rheometer data, *Polym. Eng. Sci.* **7**, 178-181.
- Bohlin VOR Rheometer Users Manual, Malvern Instruments, Westborough, MA.
- Bousmina, M., A. Ait-Kadi, and J. B. Faisant, 1999, Determination of shear rate and viscosity from batch mixer data, *J. Rheol.* **43**, 415-433.
- Bozell, J. J., L. Moens, D. C. Elliott, Y. Wang, G. G. Neuen-schwander, S. W. Fitzpatrick, R. J. Bilski, and J. L. Jarnefeld,

- 2000, Production of levulinic acid and use as a platform chemical for derived products, *Resources, Conservation and Recycling* **28**, 227-239.
- Bozell, J. J. and G. R. Petersen, 2010, Technology development for the production of biobased products from biorefinery carbohydrates-the US Department of Energy's "Top 10" revisited, *Green Chemistry* **12**, 539-554.
- Connelly, R. J. and J. L. Kokini, 2004, The effect of shear thinning and differential viscoelasticity on mixing in a model 2D mixer as determined using FEM with particle tracking, *J. Non-Newton. Fluid Mech.* **123**, 1-17.
- Dalpkke, B. and R. Kerekes, 2005, The influence of fibre properties on the apparent yield stress of flocculated pulp suspensions, *J. Pulp Paper Sci.* **31**, 39-43.
- Dodson, C. T. J., 1996, Fiber crowding, fiber contacts, and fiber flocculation, *TAPPI J.* **79**, 211-215.
- Dzuy, N. Q. and D. V. Boger, 1983, Yield stress measurement for concentrated suspensions, *J. Rheol.* **27**, 321-349.
- Dzuy, N. Q. and D. V. Boger, 1985, Direct Yield Stress Measurement with the Vane Method, *J. Rheol.* **29**, 335-347.
- Ehrhardt, M. R., 2008, Rheology of Biomass, M.S. Thesis, University of Wisconsin, Madison, WI.
- Ehrhardt, M. R., T. O. Monz, T. W. Root, R. K. Connelly, C. T. Scott, and D. J. Klingenberg, 2010, Rheology of Dilute Acid Hydrolyzed Corn Stover at High Solids Concentration, *Appl. Biochem. Biotechnol.* **160**, 1102-1115.
- Goodrich, J. E. and R. S. Porter, 1967, A rheological interpretation of torque-rheometer data, *Polym. Sci. Eng.* **7**, 45-51.
- Jorgensen, H., J. Vibe-Pedersen, J. Larsen, and C. Felby, 2007, Liquefaction of lignocellulose at high-solids concentrations, *Biotechnol. Bioeng.* **96**, 862-870.
- Kerekes, R. J., 1985, The flocculation of pulp fibers, in *Papermaking Raw Materials*, V. Punton, ed., Mechanical Engineering Publications Ltd., London, pp. 265-310.
- Kerekes, R. J. and C. J. Schell, 1992, Characterization of fibre flocculation regimes by a crowding factor, *J. Pulp. Paper Sci.* **18**, J32-J38.
- Kerekes, R. J., 1995, Perspectives on fibre flocculation in papermaking, in *1995 Proceedings of the International Paper Physics Conference*, CPPA, Montreal, pp. 23-31.
- Kerekes, R., 2006, Rheology of fibre suspensions in papermaking: An overview of recent research, *Nordic Pulp Paper Res. J.* **21**, 598-612.
- Knutsen, J. S. and M. W. Liberatore, 2009, Rheology of high-solids biomass slurries for biorefinery applications, *J. Rheol.* **53**, 877-892.
- Knutsen, J. S. and M. W. Liberatore, 2010, Rheology modification and enzyme kinetics of high solids cellulosic slurries, *Energy Fuels* **24**, 3267-3274.
- Kurath, S. F., 1959, The network and viscoelastic properties of wet pulp. I. Dynamic mechanical analysis, *Tappi* **42**, 953-959.
- Lee, P. F. W. and T. Lindstrom, 1989, Effects of high molecular mass anionic polymers on paper sheet formation, *Nordic Pulp Pap. Res. J.* **4**, 61-70.
- Lindstrom, T., 1989, Some fundamental aspects on paper forming, in *Fundamentals of Papermaking*, C. F. Baker and V. W. Punton, eds., Mechanical Engineering Publishers, Ltd., London, pp. 311-412.
- Lu, Y., Y. Wang, G. Xu, J. Chu, Y. Zhuang, and S. Zhang, 2010, Influence of high solid concentration on enzymatic hydrolysis and fermentation of steam-exploded corn stover biomass, *Appl. Biochem. Biotechnol.* **160**, 360-369.
- Lynd, L. R., 1996, Overview and evaluation of fuel ethanol from cellulosic biomass: Technology, economics, the environment, and policy, *Annu. Rev. Energy Environ.* **21**, 403-465.
- Meyer, R. and D. Wahren, 1964, On the elastic properties of three-dimensional fiber networks, *Svensk Papperstidn.* **67**, 432-436.
- Monz, T. O., 2009, Investigation of biomass rheology in different geometries, Diplomarbeit Thesis, Stuttgart University and University of Wisconsin, Madison, WI.
- Pimenova, N. and T. Hanley, 2003, Measurement of rheological properties of corn stover suspensions, *Appl. Biochem. Biotechnol.* **106**, 383-392.
- Pimenova, N. and T. Hanley, 2004, Effect of corn stover concentration on rheological characteristics, *Appl. Biochem. Biotechnol.* **114**, 347-360.
- Rosgaard, L., P. Andric, K. Dam-Johansen, S. Pedersen, and A. S. Meyer, 2007, Effects of substrate loading on enzymatic hydrolysis and viscosity of pretreated barley straw, *Appl. Biochem. Biotechnol.* **143**, 27-40.
- Samaniuk, J. R., C. T. Scott, T. W. Root, and D. J. Klingenberg, 2011, to be submitted.
- Schell, D. J., J. Farmer, M. Newman, and J. D. McMillan, 2003, Dilute sulfuric acid pretreatment of corn stover in pilot-scale reactor. Investigation of yields, kinetics, and enzymatic digestibilities of solids, *Appl. Biochem. Biotechnol.* **105**, 69-85.
- Scott, C. T., 2002, Pulp extrusion and ultra-high consistencies: selection of water-soluble polymers for process optimization, Tappi Fall Conference & Trade Fair, <http://www.fpl.fs.fed.us/documnts/pdf2002/scott02a.pdf>.
- Serrano-Ruiz, J. C., D. Wang, and J. A. Dumesic, 2010a, Catalytic upgrading of levulinic acid to 5-nonanone, *Green Chemistry* **12**, 574-577.
- Serrano-Ruiz, J. C., D. J. Braden, R. M. West, and J. A. Dumesic, 2010b, Conversion of cellulose to hydrocarbon fuels by progressive removal of oxygen, *Appl. Catalysis B: Environmental* **100**, 184-189.
- Sheehan, J., A. Aden, K. Paustian, K. Killian, J. Brenner, M. Walsh, and R. Nelson, 2004, Energy and environmental aspects of using corn stover for fuel ethanol, *J. Ind. Ecology* **7**, 117-146.
- Singh, K. M., 1985, Flow Characteristics of High Consistency Pulp as Studied in a Concentric Cylinder Viscometer, M. S. Thesis, State University of New York, Syracuse, New York.
- Soszynski, R. M. and R. J. Kerekes, 1988a, Elastic interlocking of nylon fibers suspended in liquid. Part 1. Nature of cohesion among fibers, *Nordic J. Pulp Paper Res.* **3**, 172-179.
- Soszynski, R. M. and R. J. Kerekes, 1988b, Elastic interlocking of nylon fibers suspended in liquid. Part 2. Process of interlocking, *Nordic J. Pulp Paper Res.* **3**, 180-184.
- Steffe, J. F., 1996, *Rheological Methods in Food Processing Engineering*, 2nd ed., Freeman, East Lansing.
- Stickel, J. J., J. S. Knutsen, M. W. Liberatore, W. Luu, D. W.

- Bouseld, D. J. Klingenberg, C. T. Scott, T. W. Root, M. R. Ehrhardt, and T. O. Monz, 2009, Rheology measurements of a biomass slurry: an inter-laboratory study, *Rheol. Acta* **48**, 1005-1015.
- Swerin, A., R. L. Powell, and L. Odberg, 1992, Linear and non-linear dynamic viscoelasticity of pulp fiber suspensions, *Nordic Pulp Paper Res. J.* **7**, 126-132.
- Switzer, L. H., 2002, Simulations of Systems of Flexible Fibers, Ph. D. thesis, University of Wisconsin-Madison.
- Switzer, L. H. and D. J. Klingenberg, 2003, Rheology of sheared flexible fiber suspensions via fiber-level simulations, *J. Rheol.* **47**, 759-778.
- Thalen, N. and D. Wahren, 1964a, A new elasto-viscometer, *Svensk Papperstidn.* **67**, 226-231.
- Thalen, N. and D. Wahren, 1964b, Shear modulus and ultimate shear strength of some paper pulp fiber networks, *Svensk Papperstidn.* **67**, 259-264.
- Thalen, N. and D. Wahren, 1964c, An experimental investigation of the shear modulus of model fibre networks, *Svensk Papperstidn.* **67**, 474-480.
- Um, B. and T. R. Hanley, 2008, A comparison of simple rheological parameters and simulation data for zymomonas mobilis fermentation broths with high substrate loading in a 3-L bioreactor, *Appl. Biochem. Biotechnol.* **145**, 29-38.
- Viamajala, S., J. D. McMillan, D. J. Schell, and R. T. Elander, 2009, Rheology of corn stover slurries at high solids concentrations. Effects of saccharification and particle size, *Biore-source Technology* **100**, 925-934.
- Wang, J., 2012, Ph. D. Thesis, University of Wisconsin, Madison, WI.
- Wingren, A., M. Galbe, and G. Zacchi, 2003, Techno-economic evaluation of producing ethanol from softwood: Comparison of SSF and SHF and identification of bottlenecks, *Biotechnol. Prog.* **19**, 1109-1117.
- Wooley, R., M. Ruth, J. Sheehan, K. Ibsen, H. Majdeski, and A. Galvez, 1999, Lignocellulosic biomass to ethanol process design and economics utilizing co-current dilute acid prehydrolysis and enzymatic hydrolysis current and futuristic scenarios, NREL Technical Report TP-58026157.
- Wyman, C. E., 2007, What is (and is not) vital to advancing cellulosic ethanol, *Trends in Biotechnology* **25**, 153-157.
- Zauscher, S., 1999, Polymer Mediated Surface Interactions in Pulp Fiber Suspension Rheology, Ph. D. Thesis, University of Wisconsin.
- Zauscher, S., C. T. Scott, J. L. Willet, and D. J. Klingenberg, 2000, Pulp Extrusion at ultra-high consistencies: a new processing method for recycling wastepapers and papermill sludges, *TAPPI J.* **83**, 62.
- Zauscher, S. and D. J. Klingenberg, 2000, Normal forces between cellulose surfaces measured with colloidal probe microscopy, *J. Coll. Int. Sci.* **229**, 497-510.
- Zauscher, S. and D. J. Klingenberg, 2001a, Friction forces between cellulose surfaces measured with colloidal probe microscopy, *Coll. Surf. A* **178**, 213-229.
- Zauscher, S. and D. J. Klingenberg, 2001b, Surface and friction forces between cellulose surfaces measured with colloidal probe microscopy, *Nordic Pulp Pap. Res. J.* **15**, 459-468.